

Pulse-Width Pulse-Frequency Based Optimal Controller Design for Kinetic Kill Vehicle Attitude Tracking Control

Xingyuan Xu, Yuanli Cai

Department of Automatic Control, Xi'an Jiao Tong University, Xi'an, China

E-mail: xuxingyuan2003@126.com

Received December 30, 2010; revised March 22, 2011; accepted March 25, 2011

Abstract

The attitude control problem of the kinetic kill vehicle is studied in this work. A new mathematical model of the kinetic kill vehicle is proposed, the linear quadratic regulator technique is used to design the optimal attitude controller, and the pulse-width pulse-frequency modulator is used to shape the continuous control command to pulse or on-off signals to meet the requirements of the reaction thrusters. The methods to select the appropriate parameters of pulse-width pulse-frequency are presented in detail. Numerical simulations show that the performance of the LQR/PWPF approach can achieve good control performance such as pseudo-linear operation, high accuracy, and fast enough tracking speed.

Keywords: Attitude Control, Kinetic Kill Vehicle, Linear Quadratic, Pulse-Width Pulse-Frequency

1. Introduction

It is known that the earliest interceptor required a very large and powerful propulsion system in combination with a very high powered warhead to successfully destroy an incoming reentry vehicle. With the development of small-size propulsion systems, reliable and accurate sensors and guidance systems, and rapid servo-mechanism techniques, the kinetic kill vehicle (KKV) is now becoming both technically and economically feasible. KKV adopts the way of direct collision to destroy target, which makes the promise of a low-cost defense system more reasonable. A KKV should include a sensor that identifies and tracks the target, the guidance and control system computes the course changes for the interceptor, and a propulsion system supplies the forces to maneuver the vehicle [1-3]. Each KKV requires six to eight thrusters to maneuver its pitching angle, yawing angle, and rolling angle. A procedure for finding the optimal thruster configuration with desired control effectiveness was proposed by [4].

The reaction thruster attitude control system (RTACS) has been widely studied. Aventine *et al.* [5] studied the attitude dynamics for rigid spacecraft. The firing logic of reaction thrusters and the methods of tracking attack angle are presented by He *et al.* [6], but the coupling between three channels have not been taken into account in their work. Reference [7] employed switching strategy in

combination with PID controller applying to the ducted rocket system. Luo *et al.* [8] proposed an optimization approach combining primer vector theory and evolutionary algorithms for fuel-optimal non-linear impulsive rendezvous, which is designed to seek the optimal number of impulses as well as the optimal impulse vectors. Reference [9] presented an adaptive attitude control law based on neural network for a rigid spacecraft without requiring angular velocity measurements, but in the course of this research, we found that control performance indices deteriorated obviously without tracking angular velocity. Reference [10] studied the coupled dynamics of spacecraft, and introduced angle decoupling conditions of attitude control problem.

This work adopts pulse or on-off reaction thruster for attitude maneuver. Pulse-width pulse-frequency (PWPF) modulator is used to translate continuous control commands to on-off signals due to its advantages over other types of pulse modulators such as bang-bang controller which has excessive energy consumption [11-13]. The PWPF modulator is composed of a Schmidt trigger, a first-order-filter, and a feedback loop. The design of PWPF requires iterative tuning of the filter and the Schmidt trigger. References [13-16] presented detailed methods to select the appropriate parameters of PWPF, but the relationship between signal attenuation and PWPF parameters has not been taken into account. The fuel decides the lifetime of the KKV, therefore, reduced

energy consumption is highly required, therefore, *i.e.*, decrease the number of firings.

In this work, the PWPF is combined with the linear quadratic regulator (LQR) technique for the KKV attitude control system. The paper is divided into 5 sections. The nonlinear model of the KKV is presented in Section 2; Section 3 presents a detail description of the LQR/PWPF controller design which includes the description of the tuning methods for the parameters of the PWPF modulator; Section 4 presents the result of the numerical simulation for the RTACS; Conclusions are presented in Section 5 based on the obtained results.

2. Mathematical Model of the KKV

This section will describe the mathematical model of the attitude motion, including kinematics and dynamics equations of the KKV. In general, the response, energy consumption, effective torque and fault tolerance of the control system are affected by the thruster configuration [4]. The basic thruster configuration of the KKV in this work is illustrated in **Figure 1**. There are 6 thrusters parallel to the OY_1-OZ_1 plane of the vehicle. These thrusters are installed in the tail of the KKV. Positive pitching moment is acquired by turning on thruster number 1 and 2, and negative pitching moment is acquired by turning on thruster number 4 and 5. Positive yawing moment is acquired by turning on thruster number 3, and negative yawing moment is acquired by turning on thruster number 6. Positive rolling moment is acquired by turning on thruster number 2 and 5, and negative rolling moment is acquired by turning on thruster number 1 and 4. The control commands are given in 3 channels: pitching, yawing, and rolling. Obviously, there happens control cross coupling phenomena. Smaller effective torque compared to the control command is produced when 3 channel commands are given simultaneously.

2.1. The Rotational Dynamic Equation of the KKV

In this work, the attitude of the KKV is defined by the body reference frame $OX_1Y_1Z_1$ with respect to the ground reference frame, $OX_2Y_2Z_2$ is obtained through translation of the ground reference frame and O is the center of gravity. **Figure 2** presents the relationship of the body reference frame $OX_1Y_1Z_1$ and the ground reference frame $OX_2Y_2Z_2$. For $OX_1Y_1Z_1$, OX_1 axis align with the longitudinal symmetric axis of the body, OY_1 axis and OZ_1 axis are perpendicular to OX_1 axis, and completes a three-axis right-hand orthogonal system. For $OX_2Y_2Z_2$, OX_2 axis is parallel to the plane of the ground, in the direction of the launch direc-

tion; OY_2 axis is perpendicular to the ground; OZ_2 axis is perpendicular to OX_2 and OY_2 , also completes a three-axis right-hand orthogonal system.

The motions of the KKV are composed of translational and rotational motions. Their independent characteristics allow one to deal with the two motions separately. For attitude control, only rotational equations are required. The rotational motions of a rigid spacecraft in space are described by Euler's Equation (1)

$$\frac{d\mathbf{H}}{dt} = \frac{\partial \mathbf{H}}{\partial t} + \boldsymbol{\omega} \times \mathbf{H} = \mathbf{M} \quad (1)$$

here $\boldsymbol{\omega} = (\omega_{x_1}, \omega_{y_1}, \omega_{z_1})^T$ is the angular velocity of the body frame relative to the ground frame, and the projection of $\boldsymbol{\omega}$ in the body reference frame are $\omega_{x_1}, \omega_{y_1}$ and ω_{z_1} respectively; $\mathbf{H} = \mathbf{J} \cdot \boldsymbol{\omega}$ is the moment of momentum, and \mathbf{J} is the inertia matrix. Suppose the KKV in this work is an axis-symmetric vehicle, thus the product of inertia in \mathbf{J} is zero. J_{x_1} , J_{y_1} and J_{z_1} are the moment of inertia relating to body axes. \mathbf{M} represents the control torques used for controlling the attitude. M_{x_1} , M_{y_1} and M_{z_1} are the control torques about the body axes which is provided by the thrusters.

The moment of momentum can be expressed as

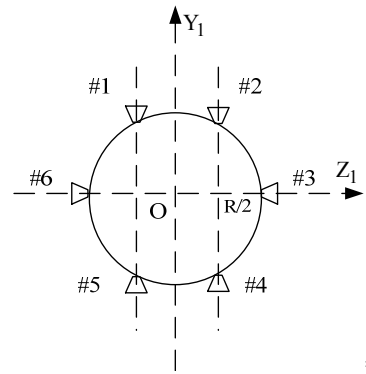


Figure 1. Configuration of attitude control thrusters.

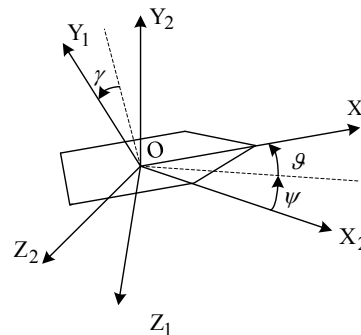


Figure 2. Relationship of the body reference frame and the ground reference frame.

$$\mathbf{H} = \mathbf{J} \cdot \boldsymbol{\omega} = \begin{bmatrix} J_{x_1} & 0 & 0 \\ 0 & J_{y_1} & 0 \\ 0 & 0 & J_{z_1} \end{bmatrix} \begin{bmatrix} \omega_{x_1} \\ \omega_{y_1} \\ \omega_{z_1} \end{bmatrix} = \begin{bmatrix} J_{x_1} \omega_{x_1} \\ J_{y_1} \omega_{y_1} \\ J_{z_1} \omega_{z_1} \end{bmatrix} \quad (2)$$

$$\frac{\partial \mathbf{H}}{\partial t} = \begin{bmatrix} J_{x_1} \frac{d\omega_{x_1}}{dt} \\ J_{y_1} \frac{d\omega_{y_1}}{dt} \\ J_{z_1} \frac{d\omega_{z_1}}{dt} \end{bmatrix} \quad (3)$$

$$\boldsymbol{\omega} \times \mathbf{H} = \begin{bmatrix} (J_{z_1} - J_{y_1}) \omega_{z_1} \omega_{y_1} \\ (J_{x_1} - J_{y_1}) \omega_{x_1} \omega_{z_1} \\ (J_{y_1} - J_{x_1}) \omega_{y_1} \omega_{x_1} \end{bmatrix} \quad (4)$$

The control torques about the body axes are

$$\mathbf{M} = \begin{bmatrix} M_{x_1} \\ M_{y_1} \\ M_{z_1} \end{bmatrix} = \begin{bmatrix} T_{x_1} R \\ T_{y_1} L \\ T_{z_1} L \end{bmatrix} \quad (5)$$

where R is the radius of the body; L is the distance from the location of thruster to the center of mass; T_{x_1} , T_{y_1} and T_{z_1} are the thruster force in different directions.

According to (1-5), the rotational dynamic equation of KKV can be expressed as

$$\begin{cases} \dot{\omega}_{x_1} = [(J_{y_1} - J_{z_1}) \omega_{y_1} \omega_{z_1} + T_{x_1} R] / J_{x_1} \\ \dot{\omega}_{y_1} = [(J_{z_1} - J_{x_1}) \omega_{z_1} \omega_{x_1} + T_{y_1} L] / J_{y_1} \\ \dot{\omega}_{z_1} = [(J_{x_1} - J_{y_1}) \omega_{x_1} \omega_{y_1} + T_{z_1} L] / J_{z_1} \end{cases} \quad (6)$$

2.2. The Rotational Kinematic Equation of the KKV

According to the relationship of the body reference frame and the ground reference frame, the rotational angular velocity of KKV in body reference frame can be deduced as follow

$$\begin{bmatrix} \omega_{x_1} \\ \omega_{y_1} \\ \omega_{z_1} \end{bmatrix} = L_x(\gamma) L_z(\vartheta) \begin{bmatrix} 0 \\ \dot{\psi} \\ 0 \end{bmatrix} + L_x(\gamma) \begin{bmatrix} 0 \\ 0 \\ \dot{\vartheta} \end{bmatrix} + \begin{bmatrix} \dot{\gamma} \\ 0 \\ 0 \end{bmatrix}$$

$$= \begin{bmatrix} \dot{\psi} \sin \vartheta + \dot{\gamma} \\ \dot{\psi} \cos \vartheta \cos \gamma + \dot{\vartheta} \sin \gamma \\ -\dot{\psi} \cos \vartheta \sin \gamma + \dot{\vartheta} \cos \gamma \end{bmatrix}$$

$$= \begin{bmatrix} 1 & \sin \vartheta & 0 \\ 0 & \cos \vartheta \cos \gamma & \sin \gamma \\ 0 & -\cos \vartheta \sin \gamma & \cos \gamma \end{bmatrix} \begin{bmatrix} \dot{\gamma} \\ \dot{\psi} \\ \dot{\vartheta} \end{bmatrix} \quad (7)$$

where ϑ , ψ and γ are pitching angle, yawing angle and rolling angle respectively, then we obtain

$$\begin{cases} \dot{\vartheta} = \omega_{y_1} \sin \gamma + \omega_{z_1} \cos \gamma \\ \dot{\psi} = (\omega_{y_1} \cos \gamma - \omega_{z_1} \sin \gamma) / \cos \vartheta \\ \dot{\gamma} = \omega_{x_1} - (\omega_{y_1} \cos \gamma - \omega_{z_1} \sin \gamma) \tan \vartheta \end{cases} \quad (8)$$

3. Design of LQR/PWPF Controller

In this section, the LQR/PWPF controller design is described. LQR is a method for designing optimal controller. However, the control signals from LQR controller are of continuous type, the PWPF is used to modulate continuous control commands to discrete signals.

3.1. LQR Controller

According to (6) and (8), the rotational dynamic and kinematic equation groups of KKV have the characteristic of strong coupling and nonlinearity. Only linearized reasonably, RTACS can use linear system theory. Suppose the attitude angle and angular velocity of KKV are all small, we can consider RTACS as a three-axis self-governed second-order linear model, and it is linearized and decoupled in the following section.

Pitching channel

$$\begin{cases} \dot{\vartheta} = \omega_{z_1} \\ \dot{\omega}_{z_1} = (T_{z_1} L) / J_{z_1} = k_z u_z \end{cases} \quad (9)$$

Yawing channel

$$\begin{cases} \dot{\psi} = \omega_{y_1} \\ \dot{\omega}_{y_1} = (T_{y_1} L) / J_{y_1} = k_y u_y \end{cases} \quad (10)$$

Rolling channel

$$\begin{cases} \dot{\gamma} = \omega_{x_1} \\ \dot{\omega}_{x_1} = (T_{x_1} L) / J_{x_1} = k_x u_x \end{cases} \quad (11)$$

In (9-11), u_x , u_y and u_z are the thruster control signal in three different channel; k_x , k_y and k_z are coefficients of u_x , u_y and u_z .

The three channels can be expressed by a second-order system

$$\begin{cases} \dot{\mathbf{x}}_1(t) = \mathbf{x}_2(t) \\ \dot{\mathbf{x}}_2(t) = \mathbf{k} \mathbf{u}(t) \end{cases} \quad (12)$$

$$\mathbf{y} = \begin{bmatrix} x_1(t) \\ x_2(t) \end{bmatrix} \quad (13)$$

The problem has the following state-space representation

$$\begin{cases} \dot{\mathbf{x}} = \mathbf{A}\mathbf{x} + \mathbf{B}\mathbf{u} \\ \mathbf{y} = \mathbf{C}\mathbf{x} + \mathbf{D}\mathbf{u} \end{cases} \quad (14)$$

For the controller design, it is necessary to check the limitations and constraints imposed by the plant. The matrix $[\mathbf{A} \ \mathbf{B}]$ must be controllable and $[\mathbf{A} \ \mathbf{C}]$ must be detectable. If both conditions are satisfied for the attitude model, the next step is to design a controller which achieves the system performance required. Stable, fast regulating angle is required. It is desired to accomplish the regulation to maintain the KKV in the required attitude.

Suppose the initial and final values of the system are given in the follow

$$\begin{cases} x_1(t_0) = x_{10} \\ x_2(t_0) = x_{20} \end{cases} \quad (15)$$

By considering the state-space (14) and (15), the optimal control problem is formulated as a two point boundary value problem. In order to reduce energy consumption, we formulate the following cost function

$$\begin{aligned} J = & \frac{1}{2} \mathbf{e}^T(t_f) \mathbf{F} \mathbf{e}(t_f) \\ & + \frac{1}{2} \int_{t_0}^{t_f} [\mathbf{e}^T(t) \mathbf{Q}(t) \mathbf{e}(t) + \mathbf{u}^T(t) \mathbf{R}(t) \mathbf{u}(t)] dt \end{aligned} \quad (16)$$

where $\mathbf{e}(t)$ is the error of the expectation output $\tilde{\mathbf{y}}(t)$ and the reality output.

$$\mathbf{e}(t) = \tilde{\mathbf{y}}(t) - \mathbf{y}(t) \quad (17)$$

$$\tilde{\mathbf{y}}(t) = \begin{bmatrix} \tilde{x}_1(t) \\ \tilde{x}_2(t) \end{bmatrix} \quad (18)$$

The first term in (16) corresponds to the energy of the final error, the second term corresponds to the energy of the instantaneous error and the third term corresponds to the energy of the control signal. The weighting matrices \mathbf{F} , \mathbf{Q} and \mathbf{R} are defined the trade-off between regulation performance and control efforts [17]. \mathbf{Q} is assumed at positive definite, and \mathbf{R} is assumed at semi-positive definite. Weighting matrices should be selected according to specific control requirements. Fast regulating angle requires large control variable, and large control variable means small \mathbf{R} ; Saving fuel requires small control variable, while small control variable means large \mathbf{R} . In addition, the thruster is not a simple linear links which has

dead zone and saturation, therefore a larger matrix \mathbf{R} relative to matrix \mathbf{Q} is necessary, thus the thruster save more fuel and work more in the linear region. Smaller control variables inevitably lead to lengthen regulation time and unable to meet intercept performance indices. So it is necessary to find a compromise when choosing \mathbf{R} . The control signal $\mathbf{u}(t)$ is obtained by minimizing J in the optimization problem [18].

For infinity time fixed-length tracking system, the approximate optimal control to minimize the cost function (16) is shown below [19]

$$\hat{\mathbf{u}}(t) = -\mathbf{R}^{-1}(t) \mathbf{B}^T(t) [\hat{\mathbf{P}}\mathbf{x}(t) - \hat{\mathbf{g}}] \quad (19)$$

where $\hat{\mathbf{P}}$ is a symmetry positive constant matrix. $\hat{\mathbf{P}}$ is obtained by solving the following Riccati equation

$$\hat{\mathbf{P}}\mathbf{A} + \mathbf{A}^T \hat{\mathbf{P}} - \hat{\mathbf{P}}\mathbf{B}\mathbf{R}^{-1}\mathbf{B}^T \hat{\mathbf{P}} + \mathbf{C}^T \mathbf{Q} \mathbf{C} = \mathbf{0} \quad (20)$$

Constant concomitance vector $\hat{\mathbf{g}}$ satisfies the following equation

$$\hat{\mathbf{g}} = [\hat{\mathbf{P}}\mathbf{B}\mathbf{R}^{-1}\mathbf{B}^T - \mathbf{A}^T]^{-1} \mathbf{C}^T \mathbf{Q} \tilde{\mathbf{y}}(t) \quad (21)$$

Thus, from (14) and (19), the approximate optimal closed-loop track system is

$$\dot{\mathbf{x}}(t) = [\mathbf{A} - \mathbf{B}\mathbf{R}^{-1}\mathbf{B}^T \hat{\mathbf{P}}] \mathbf{x}(t) + \mathbf{B}\mathbf{R}^{-1}\mathbf{B}^T \hat{\mathbf{g}} \quad (22)$$

The solution that satisfies the initial condition is the approximate optimal $\mathbf{x}^*(t)$.

3.2. Pulse-Width Pulse-Frequency Modulator

Equation (19) shows the optimal attitude control commands for the KKV, however, it is of continuous type. The PWPF can modulate the continuous control command to on-off signals which meet the requirement of thrusters. In order to ensure the modulation is in a quasi-linear mode, we must modulate the width of the pulse proportionally to the magnitude of the continuous control command. In PWPF, the distance between the pulses is also modulated. Compared with other methods of modulation, the PWPF modulator has several advantages such as close-to linear operation and high accuracy, which provide scopes for the advanced control [14].

The basic structure of PWPF is shown in **Figure 3**. The PWPF modulator is composed of a Schmidt trigger which is simply an on-off relay with dead zone and hysteresis, a first-order-filter, and a negative feedback loop [15]. When a positive input to the Schmidt trigger is greater than U_{on} , the trigger output is U_m ; While the input falls below U_{off} , the trigger output is 0, and this response is also reflected for negative inputs. The error $\mathbf{e}(t)$ is the difference between the Schmidt trigger out

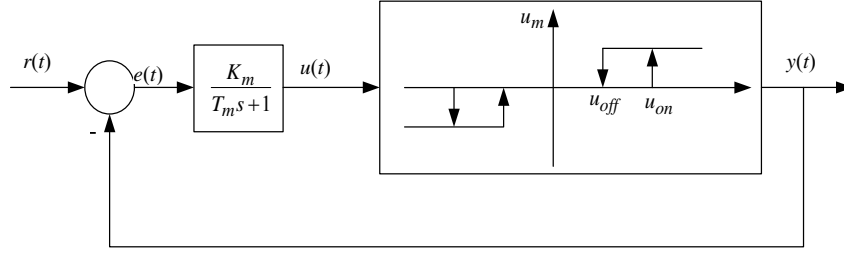


Figure 3. Pulse-width pulse-frequency (PWWF) modulator.

put U_m and the system input $r(t)$. The error is fed into the first-order-filter whose output $u(t)$ is fed to the Schmidt trigger. The parameters of interest are the first-order-filter coefficients K_m and U_m , and the Schmidt trigger parameters U_{on} and U_{off} which defines the hysteresis as $h = U_{on} - U_{off}$ (in this paper, U_m is normalized, $U_m = 1$).

3.2.1. Static Characteristics of PWWF

If the input $r(t)$ is constant, e.g., E , the PWWF modulator output on-off pulse sequence having a nearly linear duty cycle with input amplitude. It is worth to note that the modulator is independent of the system in which it is used [6]. The static characteristics indicate how the modulator will perform in most cases. Choosing appropriate static parameters of the PWWF is the first step of attitude control design.

1) On-time

The relationship between $u(t)$ and E can be represented by

$$u(t) = u(0) + [K_m(E-1) - u(0)](1 - e^{-t/T_m}) \quad (23)$$

For (23), as $t \rightarrow \infty$,

$$u(t \rightarrow \infty) = K_m(E-1) \quad (24)$$

The time from U_{on} to U_{off} is defined as the relay on-time or pulse width, denoted by T_{on} . T_{on} can be solved from (23)

$$T_{on} = -T_m \ln \left[1 + \frac{h}{K_m(E-1) - U_{on}} \right] \quad (25)$$

2) Off-time

The off-time is defined as the time from 0 to U_{on} . According to (23), the off-time denoted by T_{off} can be solved

$$T_{off} = -T_m \ln \left[1 - \frac{h}{K_mE - (U_{on} - h)} \right] \quad (26)$$

3) Modulator frequency

The frequency of the PWWF modulator is defined as the inverse of the period and is given by the following equation

$$f = \frac{1}{T_{on} + T_{off}} \quad (27)$$

4) Duty cycle

The duty cycle of PWWF is the ratio of on-time to the period and is given by

$$DC = f \times T_{on} \quad (28)$$

5) Saturation input and dead band

The maximum input E_s for pseudo-linear operation can be solved by equating the maximum value of the first-order-filter output $K_m(E_s - 1)$ to U_{off} , E_s can be determined below

$$E_s = 1 + U_{off} / K_m \quad (29)$$

The dead band of the modulator is defined as the minimum input E_d to the modulator such that $T_{on} > 0$. E_d can be determined below

$$E_d = U_{on} / K_m \quad (30)$$

From (30), we can see that increasing of K_m can reduce the size of dead band and it is reasonable to keep $K_m > 1$ to ensure that U_{on} is an upper bound of the dead band.

6) Minimum pulse-width

The effective dead band of the modulator is defined as the minimum input to the modulator when $T_{on} > 0$. Substituting (30) into (26), we obtain an expression for the minimum on-time, which is defined as the minimum pulse-width. The minimum pulse-width is usually denoted by relay operational constrains and is shown as

$$\Delta = -T_m \ln \left(1 - \frac{h}{K_m} \right) \approx \frac{hT_m}{K_m} \quad (31)$$

In addition, the normalized hysteresis width is defined as $a = h / K_m (E_s - E_d)$, and the normalized input is defined as $x = (E - E_d) / (E_s - E_d)$.

Suppose $K_m = 5$, $T_m = 0.05$, $u_{on} = 0.8$ and $h = 0.5$, then $E_d = 0.16$ and $E_s = 1.06$. The curve of static characteristics of PWWF verse input is shown in **Figure 4**. From **Figure 4**, it can be seen that when $E_d \leq E \leq E_s$, T_{on} is proportional to the input, and T_{off} is inversely

proportional to the input. The duty cycle keep a good linear relationship with input. Furthermore, when $E \leq E_d$, relay work in dead zone, and the output is zero; When $E > E_s$, relay work in saturation zone, and the output is 1. The on-off frequency varies with the input, the maximum frequency occurs at $(E_s - E_d)/2$ approximately.

3.2.2. Selection of PWWF Parameters

The aim of this section is to recommend a general method to select PWWF parameters, which will be used later for design the PWWF modulator in this work. The design is done by comparing performance indices for different parameter settings.

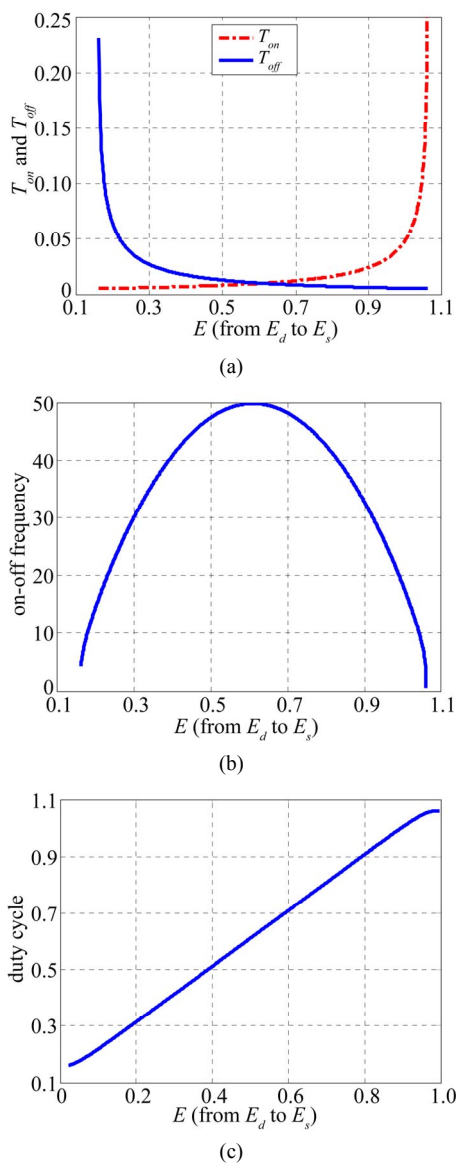


Figure 4. The curve of static characteristics of PWWF (a) T_{on} and T_{off} , (b) On-off frequency, (c) Duty cycle.

1) U_{on} and U_{off}

Simulations with a constant input $E = 0.5$ are performed to study the influence of parameters U_{on} and U_{off} on the on-off frequency. **Figure 5** illustrates the on-off frequency verse U_{on} and U_{off}/U_{on} . It indicates that for $U_{off}/U_{on} > 0.6$, the on-off frequency increases much faster than it does for $U_{off}/U_{on} < 0.6$, and for $U_{on} < 0.3$ the on-off frequency increases much faster than it does for $U_{on} > 0.3$. To avoid excessive on-off frequency, $U_{on} > 0.3$ and $U_{off}/U_{on} < 0.6$ are suggested in PWWF modulator designs.

2) K_m

A large number of simulations indicate that K_m is an important parameter which affects performance indices of PWWF. Selection of K_m is presented in detail below.

Suppose $T_m = 0.05$, $u_{on} = 0.8$ and $h = 0.5$, the influence of K_m is discussed in two cases: $K_m = 1$ and $K_m = 5$. When $K_m = 1$, we obtain $E_d = 0.8$ and $E_s = 1.3$; When $K_m = 5$, we obtain $E_d = 0.16$ and $E_s = 1.06$. The curve of the on-off frequency verse input is shown in **Figure 6**. The maximum frequency is 9 and 50 respectively. The random signal and its corresponding discrete one after PWWF are shown in **Figure 7**. From **Figure 6** and **Figure 7**, it can be seen that the smaller the K_m , the smaller the maximum frequency which means K_m is as small as possible.

PWWF translates continuous signal to discrete one, however, the process bring about changes of the signal energy. In order to study how the parameters of PWWF influence the signal energy, integral continuous signal and its corresponding discrete one respectively. Suppose the input signal is sinusoidal signal. The integral of sinusoidal signal and its discrete one after PWWF are shown in **Figure 8**. From **Figure 8**, it can be concluded that the larger K_m lead to smaller energy loss. In this sense, the larger K_m is preferred.

According to above discussion, there should be a tradeoff when choosing K_m . Simulations with varying K_m show that $1 < K_m < 6$ should be maintained.

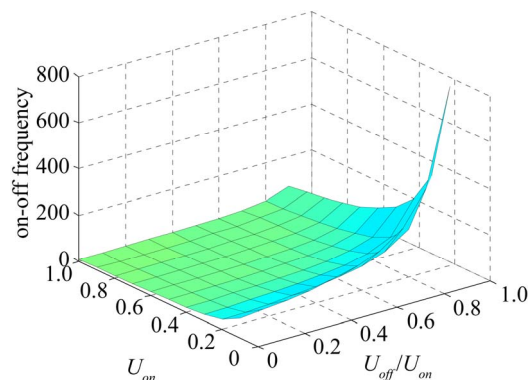


Figure 5. The on-off frequency verse U_{on} and U_{off}/U_{on} .

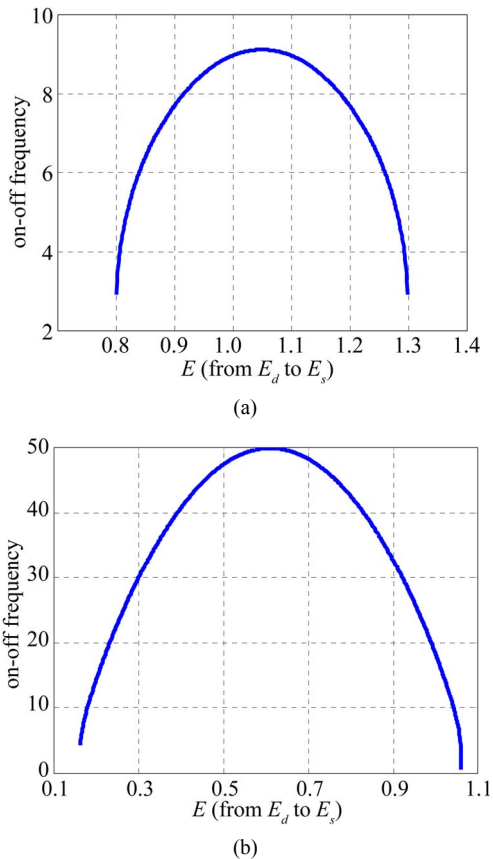


Figure 6. On-off frequency curve of PWPF (a) $K_m = 1$, (b) $K_m = 5$.

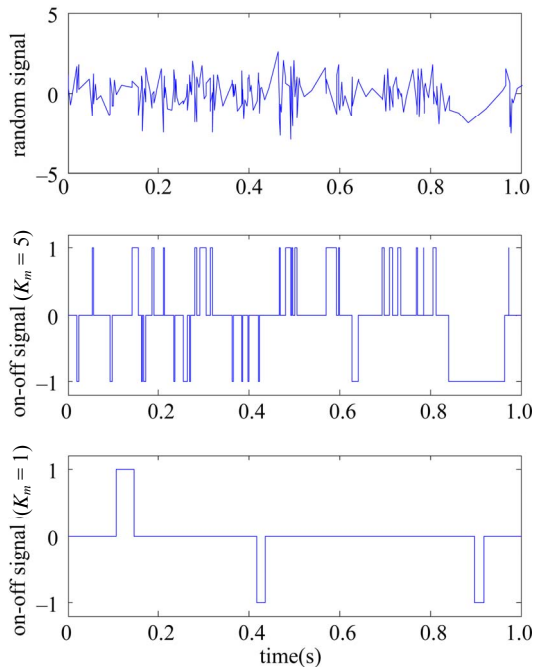


Figure 7. The random signal and its corresponding discrete signal after PWPF when $K_m = 1$ and $K_m = 5$.

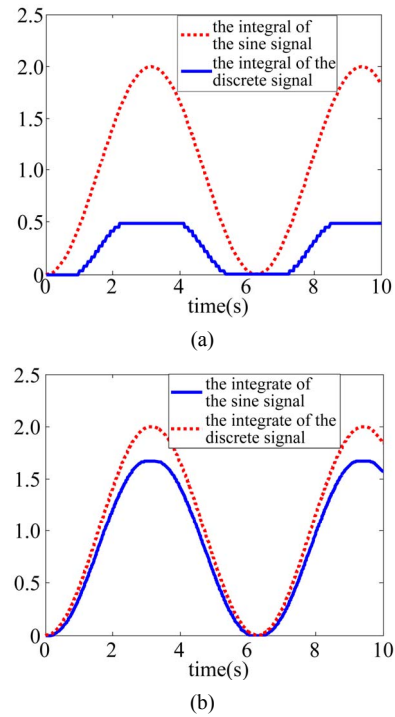


Figure 8. The integral of sinusoidal signal and its discrete signal after PWPF (a) $K_m = 1$, (b) $K_m = 5$.

3) T_m

T_m indicates a phase lag of an input. If T_m is too small, there is little phase lag for all input frequencies, and bring about excessive energy consumption; If the time constant is too large, there will be no firing numbers for the modulator to react to the high-frequency input [14].

Generally, better control performance requires larger control command, *i.e.*, requires more energy consumption, but the fuel is limited in KKV, and the number of firings gives an indication of the life-time of the thrusters. In the case of meeting the control requirements, we must minimize the number of firings, *i.e.*, minimize the firing frequency. This tradeoff has to be kept in mind during the design of the PWPF. In order to reduce the energy consumption, an iterative searching of the tradeoff can be carried out, and all the involved requirements should be satisfied. The preferred range of parameters for PWPF is recommended in **Table 1**.

Table 1. The preferred range of PWPF parameters.

Parameter	Recommended setting
Modulator gain, K_m	$1 \leq K_m \leq 6$
On-threshold, U_{on}	$U_{on} > 0.3$
Off-threshold, U_{off}	$U_{off} < 0.6 U_{on}$
Time constant, T_m	$0.02 < T_m < 0.2$

4. Numerical Results

According to above analysis, the PWWF parameters for the particular problem in this work are presented in **Table 2**. **Table 3** shows the dynamic and structure parameters of the KKV in this work.

4.1. Design of Optimal Control Law

1) Pitching channel

The matrixes of the pitching channel are shown as follows

$$A = \begin{bmatrix} 0 & 1 \\ 0 & 0 \end{bmatrix}, B = \begin{bmatrix} 0 \\ k \end{bmatrix} = \begin{bmatrix} 0 \\ 150 \end{bmatrix}, C = \begin{bmatrix} 1 & 0 \\ 0 & 1 \end{bmatrix}, D = \mathbf{0}.$$

Select $Q = \begin{bmatrix} 100 & 0 \\ 0 & 1.3 \end{bmatrix}$, $R = 0.5$, according to (19-21),

we obtain

$$P = \begin{bmatrix} 11.8080 & 0.0471 \\ 0.0471 & 0.0056 \end{bmatrix} \tag{32}$$

$$g = \begin{bmatrix} 11.8080\tilde{y}_1 - 1.3\tilde{y}_2 \\ 0.0471\tilde{y}_1 \end{bmatrix} \tag{33}$$

The optimal control law is

$$u^*(t) = -14.13x_1 - 1.68x_2 + 14.13\tilde{y}_1 \tag{34}$$

2) Yawing channel

The matrixes of the yawing channel are shown as follows

$$A = \begin{bmatrix} 0 & 1 \\ 0 & 0 \end{bmatrix}, B = \begin{bmatrix} 0 \\ k \end{bmatrix} = \begin{bmatrix} 0 \\ 75 \end{bmatrix}, C = \begin{bmatrix} 1 & 0 \\ 0 & 1 \end{bmatrix}, D = \mathbf{0}.$$

Select $Q = \begin{bmatrix} 100 & 0 \\ 0 & 3 \end{bmatrix}$, $R = 0.5$, according to (19-21),

we obtain

$$P = \begin{bmatrix} 17.8565 & 0.0943 \\ 0.0943 & 0.0168 \end{bmatrix} \tag{35}$$

$$g = \begin{bmatrix} 17.8565\tilde{y}_1 - 3\tilde{y}_2 \\ 0.0943\tilde{y}_1 \end{bmatrix} \tag{36}$$

The optimal control law is

$$u^*(t) = -14.145x_1 - 2.52x_2 + 14.145\tilde{y}_1 \tag{37}$$

3) Rolling channel

The matrixes of the yawing channel are shown as follows

$$A = \begin{bmatrix} 0 & 1 \\ 0 & 0 \end{bmatrix}, B = \begin{bmatrix} 0 \\ k \end{bmatrix} = \begin{bmatrix} 0 \\ 200 \end{bmatrix}, C = \begin{bmatrix} 1 & 0 \\ 0 & 1 \end{bmatrix}, D = \mathbf{0}.$$

Select $Q = \begin{bmatrix} 100 & 0 \\ 0 & 1.5 \end{bmatrix}$, $R = 0.5$, according to (19-21),

we obtain

$$P = \begin{bmatrix} 12.5328 & 0.0354 \\ 0.0354 & 0.0044 \end{bmatrix} \tag{38}$$

$$g = \begin{bmatrix} 12.5328\tilde{y}_1 - 1.5\tilde{y}_2 \\ 0.0354\tilde{y}_1 \end{bmatrix} \tag{39}$$

The optimal control law is

$$u^*(t) = -14.16x_1 - 1.76x_2 + 14.16\tilde{y}_1 \tag{40}$$

4.2. Numerical Result

Suppose the initial values of the three attitude angles and angle velocity are all zero, the final values are all 1 rad, the tracking profile are shown in the following. **Figure 9** presents the tracking profile when the input is step signal; **Figure 10** presents the tracking profile when the input is square signal. **Figures 11-13** present the control commands of the three channels when the final values are 1 rad, 0.5 rad, 0.1 rad respectively.

Table 2. The selected PWWF parameters.

Parameter	Recommended setting
K_m	5
U_{on}	0.8
U_{off}	0.3
T_m	0.05

Table 3. Dynamic and structure parameters of attitude control system.

	Pitching channel	Yawing channel	Rolling channel
Arm of force (m)	1	1	0.2
Moment (Nm)	600	300	60
Moment of inertia (kgm ²)	4	4	0.3
Thruster force (N)	600	300	300

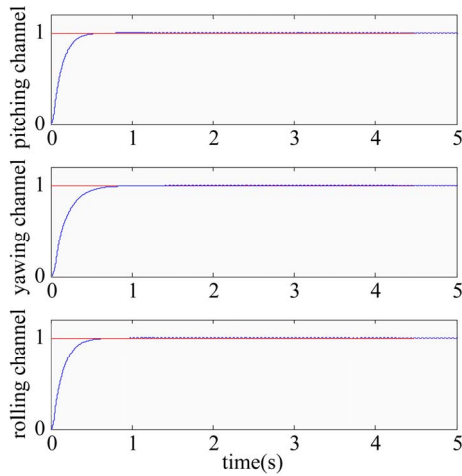


Figure 9. Attitude tracking profile when the input is step signal.

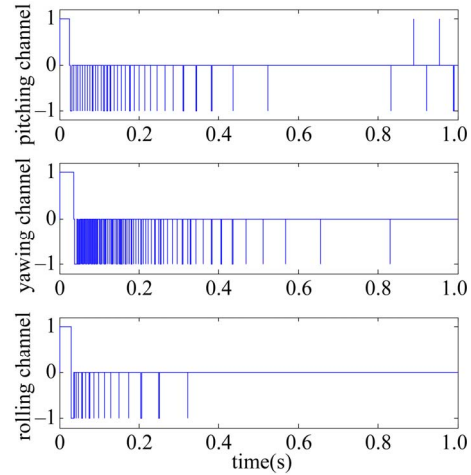


Figure 12. Control commands when inputs are 0.5 rad.

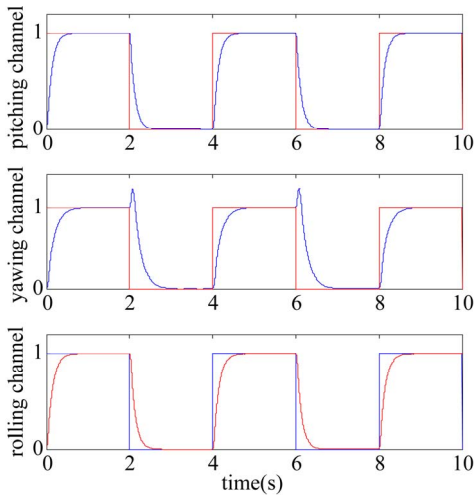


Figure 10. Attitude tracking profile when the input is square signal.

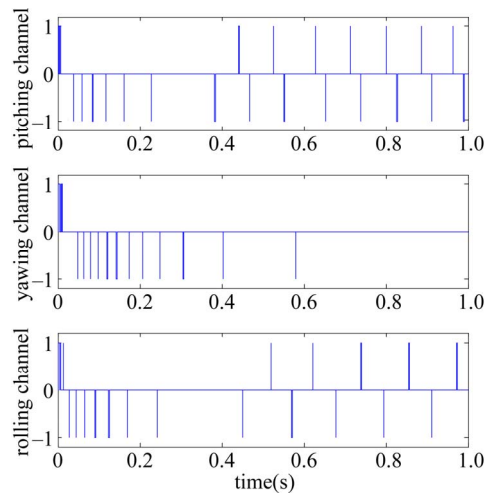


Figure 13. Control commands when inputs are 0.1 rad.

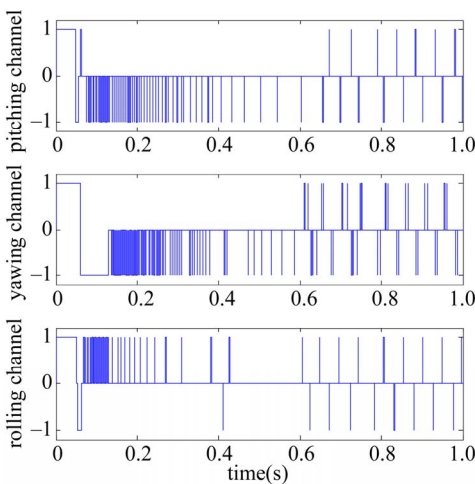


Figure 11. Control commands when inputs are 1 rad.

From the simulation results, it can be seen that there are very good tracking performance of the three attitude angles. When tracking large attitude angle, the thrusters need a high on-off frequency; when tracking small attitude angle, the thrusters reduce the number of firings. Thus, we conclude that for terminal guidance, better precision in midcourse control will reduce the number of firings in terminal phase. It is worth to note that the pitching and rolling channels share four attitude control thrusters, the two channels are coupled stronger than the yawing channel.

5. Conclusions

This work presents the design process of LQR/PWPF controller, which can meet the requirements of RTACS for KKV. Firstly, a mathematical model of RTACS for KKV is deduced. Then, the design methods of LQR and

PWPF are introduced in detail. The LQR technique is an efficient way to achieve stability; it allows to select the level of input signal, and to restrict the control commands till acceptable performance is obtained. The guidelines to select the weighting matrices of the cost function for the optimal controller are also presented and discussed in this work. The influence of PWPF modulator parameters on the control performance is studied. The analysis of the PWPF modulator presents an effective method to tune its parameters. The tuning ranges of some parameters are presented, and a set of approximate optimal parameters for the PWPF is also obtained in this work. Finally, simulation results demonstrate the feasibility of the LQR/PWPF controller for RTACS, and reasonable tracking accuracy in attitude is achieved. It is worth to note that the LQR/PWPF controller can stabilize the system for all initial states. The simulation results also show that improving the control precision in midcourse will reduce the on-off frequency of thrusters in terminal phase, and this is what we hope to achieve.

6. References

- [1] R. C. Schindler, "SDI Thinks Small-Miniaturized Propulsion is Needed for Ground- and Space-Based Kill Vehicles," *Proceedings of the 27th AIAA/SAE/ASME Joint Propulsion Conference*, AIAA Paper, No. 1991-1932, Sacramento, 1991.
- [2] J. Pavlinsky, "Advanced Thrust Chambers for Miniaturized Engines," *Proceedings of the 28th AIAA/SAE/ASME/ASEE Joint Propulsion Conference and Exhibit*, AIAA Paper, No. 1992-3258, Nashville, 1992.
- [3] E. D. Bushway and E. Nelson, "Design and Development of Lightweight Integrated Valve/Injector for the THAAD Program," *Proceedings of the 30th AIAA/SAE/ASME/ASEE Joint Propulsion Conference*, AIAA Paper, No. 1994-3383, Indianapolis, 1994.
- [4] T. W. Hwang, C. S. Park, M. J. Tahk and H. Bang, "Upper-Stage Launch Vehicle Servo Controller Design Considering Optimal Thruster Configuration," *Proceedings of AIAA Guidance, Navigation, and Control Conference and Exhibit*, AIAA Paper, No. 2003-5330, Austin, 2003.
- [5] G. Avanzini and G. Matteis, "Bifurcation Analysis of Attitude Dynamics in Rigid Spacecraft with Switching Control Logics," *Journal of Guidance, Control and Dynamics*, Vol. 24, No. 5, 2001, pp. 953-959. doi:10.2514/2.4802
- [6] H. Fenghua, M. Kemao and Y. Yu, "Firing Logic Optimization Design of Lateral Jets in Missile Attitude Control Systems," *Proceedings of the 17th IEEE International Conference on Control Applications Part of 2008 IEEE Multi-Conference on Systems and Control San Antonio*, San Antonio, 3-5 September 2008, pp. 936-941.
- [7] W. Bao, B. Li, J. Chang, W. Yu and D. Ren, "Switching Control of Thrust Regulation and Inlet Buzz Protection for Ducted Rocket," *Acta Astronautica*, Vol. 67, No. 7-8, 2010, pp. 764-773. doi:10.1016/j.actaastro.2010.04.022
- [8] Y. Z. Luo, J. Zhang, H. Y. Li and G. J. Tang, "Interactive Optimization Approach for Optimal Impulsive Rendezvous Using Primer Vector and Evolutionary Algorithms," *Acta Astronautica*, Vol. 67, No. 3-4, 2010, pp. 396-405. doi:10.1016/j.actaastro.2010.02.014
- [9] A. M. Zou and K. D. Kumar, "Adaptive Attitude Control of Spacecraft Without Velocity Measurements Using Chebyshev Neural Network," *Acta Astronautica*, Vol. 66, No. 5-6, 2010, pp. 769-779. doi:10.1016/j.actaastro.2009.08.020
- [10] Y. Wu, X. Cao, Y. Xing, P. Zheng and S. Zhang, "Relative Motion Decoupled Control for Spacecraft Formation with Coupled Translational and Rotational Dynamics," *Proceedings of the International Conference on Computer Modeling and Simulation*, 2009, pp. 63-68. doi:10.1109/ICCMS.2009.12
- [11] Q. L. Hu, "Variable Structure Maneuvering Control with Time-Varying Sliding Surface and Active Vibration Damping of Flexible Spacecraft with Input Saturation," *Acta Astronautica*, Vol. 64, No. 11-12, 2009, pp. 1085-1108. doi:10.1016/j.actaastro.2009.01.009
- [12] Q. L. Hu, "Sliding Mode Attitude Control with L2-Gain Performance and Vibration Reduction of Flexible Spacecraft with Actuator Dynamics," *Acta Astronautica*, Vol. 67, No. 5-6, 2010, pp. 572-583. doi:10.1016/j.actaastro.2010.04.018
- [13] T. D. Krovel, "Optimal Tuning of PWPF Modulator for Attitude Control," M.S. Thesis, Department of Engineering Cybernetics, Norwegian University of Science and Technology, Trondheim, 2005.
- [14] G. Song, N. V. Buck and B. N. Agrawal, "Spacecraft Vibration Reduction Using Pulse-Width Pulse-Frequency Modulated Input Shaper," *Journal of Guidance, Control and Dynamics*, Vol. 22, No. 3, 1999, pp. 433-440. doi:10.2514/2.4415
- [15] G. Song and B. N. Agrawal, "Vibration Suppression of Flexible Spacecraft During Attitude Control," *Acta Astronautica*, Vol. 49, No. 2, 2001, pp. 73-83.
- [16] G. Arantes, L. S. Martins-Filho and A. C. Santana, "Optimal On-off Attitude Control for the Brazilian Multimission Platform Satellite," *Mathematical Problems in Engineering*, Vol. 2009, No. 1, 2009, pp. 1-17. doi:10.1016/S0094-5765(00)00163-6
- [17] B. D. Anderson and J. B. Moore, "Optimal Control: Linear Quadratic Methods," Prentice Hall, Englewood Cliffs, 1990.
- [18] R. Bevilacqua, T. Lehmann and M. Romano, "Development and Experimental of LQR/APF Guidance and Control for Autonomous Proximity Maneuvers of Multiple Spacecraft," *Acta Astronautica*, Vol. 68, No. 7-8, 2011, pp. 1260-1275.
- [19] G. Y. Tang, "Suboptimal Control for Nonlinear Systems: A Successive Approximation Approach," *Systems & Control Letters*, Vol. 54, No. 5, 2005, pp. 429-434. doi:10.1016/j.sysconle.2004.09.012